Chemico-Biological Interactions 351 (2022) 109764

Contents lists available at ScienceDirect

Chemico-Biological Interactions

journal homepage: www.elsevier.com/locate/chembioint

Interactions of human acetylcholinesterase with phenyl valerate and acetylthiocholine: Thiocholine as an enhancer of phenyl valerate esterase activity

Jorge Estévez *, Marina Terol, Miguel Ángel Sogorb, Eugenio Vilanova

Nstitute of Bioengineering, University Miguel Hernández, Elche (Alicante), Spain

ARTICLE INFO

Keywords:
Human acetylcholinesterase
Phenyl valerate
Thiocholine
Inhibition kinetics
Acetylthiocholine

ABSTRACT

Phenyl valerate (PV) is a neutral substrate for measuring the PVase activity of neuropathy target esterase (NTE), a key molecular event of organophosphorus-induced delayed neuropathy. This substrate has been used to discriminate and identify other proteins with esterase activity and potential targets of organophosphorus (OP) binding. A protein with PVase activity in chicken (model for delayed neurotoxicity) was identified as butyrylcholinesterase (BChE). Further studies in human BChE suggest that other sites might be involved in PVase activity. From the theoretical docking analysis, other more favorable sites for binding PV related to the Asn289 residue located far from the catalytic site ("PVsite") were deduced.In this paper, we demonstrate that acetylcholinesterase is also able to hydrolyze PV. Robust kinetic studies of interactions between substrates PV and acetylthiocholine (AtCh) were performed. The kinetics did not fit the classic competition models among substrates. While PV interacts as a competitive inhibitor in AChE activity, AtCh at low concentrations enhances PVase activity and inhibits this activity at high concentrations. Kinetic behavior suggests that the potentiation effect is caused by thiocholine released at the active site, where AtCh could act as a Trojan Horse. We conclude that the products released at the active site could play an important role in the hydrolysis reactions of different substrates in biological systems.

1. Introduction

Cholinesterases hydrolyze acetylcholine, which are serine hydrolases present in most living beings. Acetylcholinesterase (AChE) and butyrylcholinesterase (BChE) are the most important examples of cholinesterases in vertebrates [1]. The principal biological role of AChE (acetylcholine hydrolase, EC 3.1.1.7) is the termination of impulse transmissions at cholinergic synapses by the rapid hydrolysis of neurotransmitter acetylcholine (ACh) to yield acetic acid and choline [2]. For this reason, many studies about AChE have been conducted, in which interactions with a huge number of substrates and inhibitors have been studied. The design of its active site is the cause of its observed specificity, where the catalytic triad is located at the bottom of a narrow 20 Å deep gorge [3]. The following binding sites have been described in AChE:

Esteratic site. The esteratic site is the catalytic subsite localized in the active site, which contains the three residues of the catalytic triad Ser-203, His-447, and Glu-334 [3,4]. The cholinesterase-catalyzed substrate hydrolysis takes place at the serine-containing esteratic site [5].

Anionic site (choline-binding pocket). The 'anionic' subsite (also known as cationic-π site) is localized in the active site and it interacts with the charged quaternary group of the choline moiety of ACh [6–9] accommodating the positive pole of ACh [4] and binds quaternary ligands that serve as competitive inhibitors [10]. It is formed by Trp-86 [11].

Peripheral anionic site (PAS). The PAS is localized on the AChE surface around the cavity entrance [12] at approximately 20A from the active site [13,14]. The PAS is formed by Tyr 72, Asp 74, Tyr 124, Trp 286 and Tyr 341 [14]. In a first step, the substrate provisionally interacts with the PAS in the catalytic pathway, which enhances catalytic efficiency while the substrate is captured on its way to the active site. However, substrate inhibition is observed at high substrate concentrations [14], where acetylthiocholine interacts with Asp74 of the PAS [15]. Furthermore, the PAS is related to the interactions with uncompetitive or non-competitive inhibitors [13,14,16].

Phenyl valerate (PV) is the substrate used to identify and characterize neuropathy target esterase (NTE) [17–22], the starting enzyme of

* Corresponding author.
E-mail address: jorge.estevez@umh.es (J. Estévez).

https://doi.org/10.1016/j.cbi.2021.109764
Received 20 July 2021; Received in revised form 11 November 2021; Accepted 25 November 2021
Available online 4 December 2021

Abbreviations

AtCh	acetylthiocholine
ACh	acetylcholine
AChE	acetylcholinesterase (generally of any species)
BChE	butyrylcholinesterase (generally of any species)
tCh	thiocholine
Ch	choline
ChE	cholinesterase (activity)
NTE	neuropathy target esterase
PV	phenyl valerate
PVase	phenyl valerate esterase (activity)
hAChE	human acetylcholinesterase

organophosphate-induced delayed neuropathy (OPIDN), and other serine hydrolases of neural tissue and brain [23–28]. It is a neutral (non charged) substrate like phenyl acetate.

In a soluble brain fraction of chicken, three enzymatic components of phenylvalerate esterase (PVase) activity (Eα, Eβ and Eγ) have been discriminated using irreversible inhibitors as follows: mipafox (OPIDN-inducer), paraoxon (non OPIDN-inducer) and phenylmethylsulfonyl fluoride (PMSF) [29]; 2012). Benabent et al. [30] have shown that PV (the substrate of PVase activity) partially inhibits ChE activity in soluble brain fractions of chicken, and *vice versa*, while acetylthiocholine (AtCh) displays inhibition in some PVase activity components. This scenario suggests that PVase components may contain enzymes that hydrolyze ACh. A proteomic analysis has been demonstrated that a fraction enriched with the Eα component of PVase activity contains BChE [31].

We have reported [32] that purified human BChE (hBChE) also presents PVase activity and demonstrates that a relation between hBChE and PVase activities is also relevant for humans as is, therefore, the potential role in toxicity for humans. We have demonstrated that PV and AtCh are hydrolyzed at the same time in hBChE [33]. Our results showed that the interaction between both substrates in hBChE is not compatible with a simple competition model between the substrates at the same active site, and the competition between those two substrates is not total, but is partial competition, and can be directed through the interaction at another different site to the active site. Our docking studies and molecular dynamic simulations in hBChE described how it was compatible with interactions at a site related to residue Asn298, which is far from the catalytic site. We named it the "PV-site" because the best energetically favorable poses are related to this site in theoretical docking studies [33].

In this work, we test and demonstrate that recombinant hAChE is also able to hydrolyze PV. The relation between the catalytic center of PVase activity and its AtCh hydrolyzing activity is evaluated by assessing the interactions between substrates and kinetics of the interaction between either substrates or products. These observations suggest that hAChE cannot be excluded from the pool of OP-sensitive proteins with PVase activity.

2. Materials and methods

2.1. Chemicals

Sodium dodecyl sulfate (SDS; purity 99%) was obtained from Panreac Química S.L.U. (Barcelona, Spain). Ellman's reagent, 5,5′-dithiobis-2-nitrobenzoate (DTNB, purity 99%), AtCh iodide (purity ≥98) were purchased from Sigma (Madrid, Spain), tCh iodide was obtained from BOC Sciences, and ACh iodide and Ch chloride were supplied by Sigma (Madrid, Spain). PV was attained from Lark Enterprise (Webster, MA, USA) and was checked in our laboratory by GC/MS. It contained less than 0.1% phenol and under 1% of other carboxylesters as impurities. All the other reagents were obtained from Merck SL (Madrid, Spain) and were of analytical grade.

2.2. Solutions

"Phosphate buffer", which is mentioned throughout, contained 0.1 M phosphate, pH 7.4, and 1 mM EDTA.

A stock solution of substrate PV (150 mM) was prepared in dried N, *N*-diethylformamide, and was diluted in water at the concentrations indicated in each assay immediately before the enzymatic assays. AtCh iodide, tCh iodide, ACh iodide and Ch chloride were prepared in water before being used at the concentrations indicated in each assay immediately before the enzymatic assays.

In order to stop the enzymatic reaction and color development, the following solutions were prepared: SDS-AAP solution (for PVase activity): 2% SDS (sodium dodecyl sulfate) that containing 1.23 mM of aminoantypirine in phosphate buffer. SDS-DTNB solution (for ChE activity): 2% SDS solution containing 6 mM of DTNB in phosphate buffer.

2.3. Enzyme

Recombinant hAChE was obtained from R&D Systems. hBChE was isolated from human plasma, a gift from Dr. David Lenz and Dr. Douglas Cerasoli [USAMRICD (US Army Medical Research Institute of Chemical Defense), Aberdeen Proving Ground, MD, U.S.A.]. Horse BChE and electric eel AChE came from Sigma-Aldrich.

2.4. Measuring esterase activities

2.4.1. General strategy

PVase and ChE activities were both inhibited and measured by a similar strategy and procedure to enable the comparison of the response to inhibitors and to evaluate the interaction between substrates under comparable conditions. Enzyme preparations were incubated with the substrate (PV for PVase or AtCh for ChE activity) and the reaction was stopped after the reaction time by adding a mixture containing SDS, plus the color reagent (SDS-AAP plus potassium ferricyanide for PVase activity or SDS-DTNB for ChE activity).

An automated Work Station (Beckman Biomek 2000) was employed for the pipetting and incubating process with inhibitors and substrates. Product formation (phenol or tCh) was measured by reading absorbance (510 nm or 410 nm, respectively). The specific procedures were as follows and all the measurements taken in triplicate.

2.4.2. Experiments of activities versus substrate concentration

2.4.2.1. PVase activity. PVase activity was measured according to Mangas et al. [29] by following a procedure based on the colorimetric method for the NTE assay developed by Johnson [34]. A 120 μl volume of enzyme preparation 10 nM hAChE was incubated with 120 μl of PV in a microtube at the concentration indicated in each experiment. The mixture was incubated for 5 min and 25 s at 37 °C. The enzymatic reaction was stopped by adding 120 μl of SDS-AAP solution after mixing. Then 60 μl of 1.21 mM potassium ferricyanide were added and left for color development for 5 min. A 300 μl volume from each microtube was transferred to a 96-well microplate and absorbance was read at 510 nm to estimate the phenol concentration. Blanks (buffer without hAChE) were tested for spontaneous hydrolysis by the same procedure.

2.4.2.2. ChE activity. Assays were carried out according to Benabent et al. [30]. First, 120 μl volume samples of enzyme preparation 0.1 nM hAChE (or buffer in blanks) were incubated with 120 μL of AtCh in ultrapure water in a microtube at the concentration indicated in each experiment for 5 min and 25 s at 37 °C. The enzymatic reaction was stopped by adding 120 μl of SDS-DTNB solution. Then 120 μL of

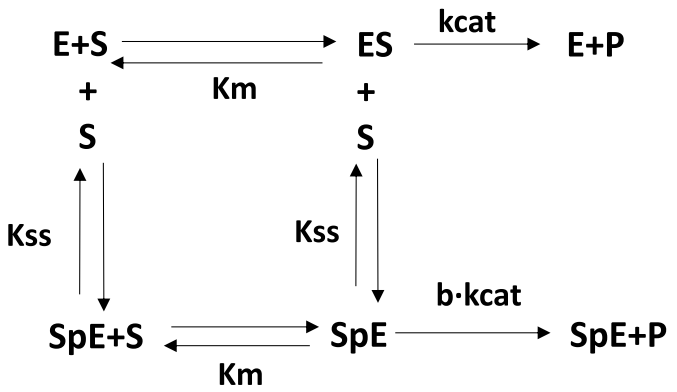

Fig. 1. - Scheme of the biphasic substrate inhibition reaction (Haldane-Radić enzymic mechanism). Km and Kss are the dissociation constants in this reaction, kcat is the catalytic constant of the non inhibited enzyme and b·kcat is the catalytic constant of the inhibited enzyme.

phosphate buffer (or diluted enzyme preparation in blanks) were added. The final assay volume was 480 μL. After mixing and waiting for at least 5 min, a 300 μL volume from each microtube was transferred to a 96-well microplate to read absorbance at 410 nm to estimate the tCh that was formed as the result of the reaction.

2.4.3. *Experiments of activities versus reaction time*

These experiments were performed similarly to those indicated in Section 2.4.1, but by modifying the reaction times with substrates. The specific procedures were as follows:

2.4.3.1. PVase activity. For each tested condition, 90 μl enzyme preparation of 10 nM of hAChE (buffer in blanks for spontaneous hydrolysis) were incubated with 90 μl of either 3 mM of PV or 3 mM PV plus (a) AtCh, (b) tCh, (c) acetate (Ac), (d) tCh plus Ac, (e) ACh or (d) Ch. Concentrations were indicated in each experiment. The mixture was incubated for the different times indicated in each experiment at 37 °C. The enzymatic reaction was stopped by adding 90 μl of SDS-AAP solution. After mixing, 45 μl of 1.21 mM potassium ferricyanide were added and left for color development for 5 min. A 250 μl volume from each microtube was transferred to a 96-well microplate. Absorbance was read at 510 nm to measure phenol formation.

2.4.3.2. ChE activity. For each tested condition, 90 μl volume samples of enzyme preparation 10 nM of hAChE (buffer in blanks) were incubated in a microtube with 90 μL of 0.5 or 0.75 mM of AtCh in ultrapure water for the different times indicated in each experiment at 37 °C. The enzymatic reaction was stopped by adding 90 μl of SDS-DTNB solution. Then 90 μL of phosphate buffer (or enzyme preparation in blanks) were added. The final assay volume was 360 μL. After mixing and waiting for at least 5 min, a 250 μL volume from each microtube was transferred to a 96-well microplate and absorbance was read at 410 nm to measure tCh formation.

2.5. *Mathematical models and kinetic data analysis*

2.5.1. *General approach*

The results of the kinetic experiments were processed by version 14 of the SigmaPlot software (Systat Software Inc, Chicago, USA) for Windows®. Non linear regression was used with the Enzyme Kinetics Module to obtain the best fitting kinetic model and to calculate the kinetic parameters. The equations describing the kinetics for the substrate reactions (Hill, Michaelis-Menten, activation by substrate, inhibition by substrate, iso-enzyme and biphasic substrate activation or inhibition) were employed to fit datasets. Competition between substrates data were analyzed with the mathematical models developed by Estevez et al.

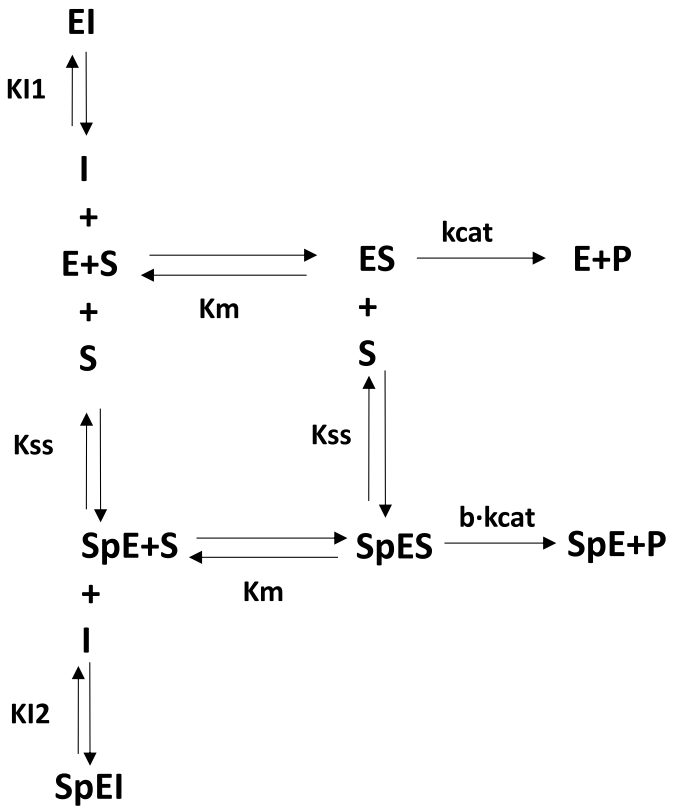

Fig. 2. Model of competitive inhibition at a low substrate concentration and a high substrate concentration. V1 = kcat·E0; V2 = α·kcat·E0; K_M, Kss, K_{I1}, and K_{I2} are the dissociation constants, while kcat is the catalytic constant.

[33]; which considered the biphasic reaction of substrate activation or inhibition and the other substrate is contemplated like a reversible inhibitor of the hydrolyzing activity. The best fitting model was established by comparing different models (Akaike, 1974) and by selecting the best fitting one with the software facilities. This procedure appears extensively in the literature [33,35–37].

2.5.2. *Model of inhibition by excess substrate*

This behavior of acetylcholinesterases, with excess substrate that does not follow the Michaelis-Menten kinetics, is usually explained by the reaction model, as shown in Fig. 1.

The reaction model, in which substrate molecule S binds to two different (active and peripheral) sites with two dissociation constants (K_m and K_{ss}), can be used to describe substrate inhibition at high substrate concentrations.

The substrate can be bound to either the free enzyme or the ES Michaelis complex. This mechanism (Fig. 1) was proposed by Radić et al. [38] for general mechanism of cholinesterases with its substrates. The mathematical model equation from this mechanism is shown in Equation (1), where V_1 is the maximum rate of the non inhibited enzyme and V_2 is the maximum rate of the enzyme inhibited by excess of substrate. This equation was shown by Cauet et al. [39] and used by other authors in BChE studies [40]. We show the mathematical derivation of this equation from the mechanism (Fig. 1) in Supplementary Material. This derivation assumes that Kss⋙Km because the affinity of the substrate by the allosteric site is much lower than the affinity of the active site.

$$v = \frac{V_1 \cdot S + V_2 \frac{S^2}{Kss}}{Km + S + \frac{S^2}{Kss}} \quad (1)$$

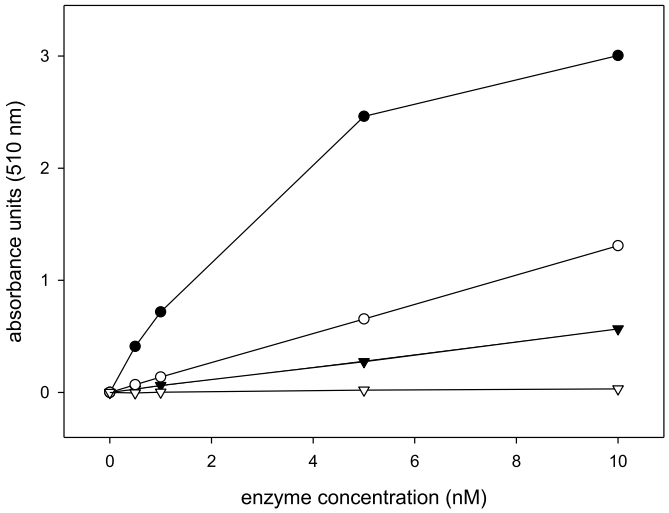

Fig. 3. - PVase activities of several cholinesterases. Several concentrations (0.5, 1, 5, 10 nM) of hBChE (black circles), hAChE (white circles), horse BChE (black triangles) and electric eel AChE (white triangles) assayed with 7.5 mM of PV for up to 10 min at 37 °C.

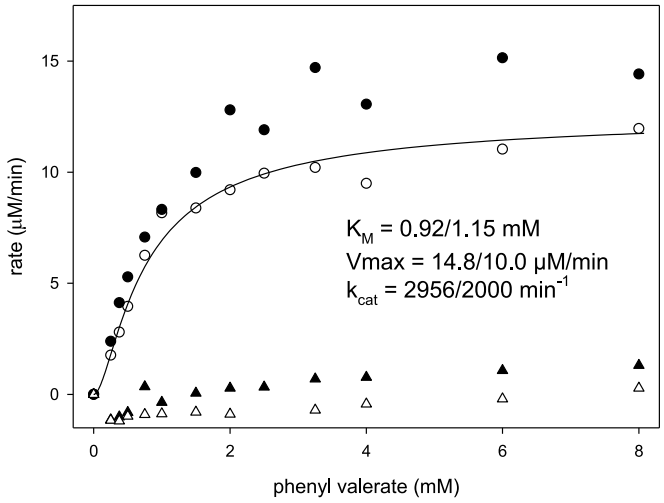

Fig. 4. PVase activity of hAChE in the presence of AtCh and kinetic parameters. One example of the two performed independent experiments is shown. AtCh concentrations: 0 (white circles), 0.5 (black circles), 3.0 (black triangles) and 20 mM (white triangles). The line shows the best fit according to Akaike's criterion (Michaelis-Menten model). The kinetic parameters of two independent experiments are shown.

2.6. Models when a substrate is considered to be the inhibitor of the hydrolyzing activity of the other substrate

Several models included by default in the Enzyme Kinetic Module of the Sigma Plot (Systat Software Inc, Chicago, USA) were tested. The best fits were deduced according to Akaike's criterion.

We deduced more than 80 different model equations of reversible inhibition to fit them to the experimental data of AtCh hydrolyzing activity in the presence of PV [33].

These model equations took into account that the AtCh hydrolyzing activity of hAChE was inhibited in the excess of AtCh. Therefore, the different kinds of reversible inhibition (full and partial competitive, full and partial uncompetitive, full and partial non competitive and full and partial mixed inhibitions) were considered in both the substrate non inhibited enzyme and the substrate-inhibited enzyme. All these models were evaluated by processing and analyzing data by adapting the model equation with the Enzyme Kinetic Module of the commercial Sigma Plot software.

The best model that fitted to our data was competitive inhibition when the enzyme was non-inhibited and inhibited by the substrate. Therefore, the data in the Results are shown using this model (Fig. 2), whose model equation is Equation (2) (see Supplementary Material for mathematical derivation).

$$V = \frac{V1 + \frac{V2 \cdot S}{Kss}}{\frac{Km}{S} + \frac{Km \cdot I}{S \cdot KI1} + \frac{Km \cdot I}{Kss \cdot KI2} + 1 + \frac{Km}{Kss} + \frac{S}{Kss}} \quad (2)$$

3. Results

3.1. PV hydrolysis by hAChE

Several cholinesterases at concentrations within the 0.5–10 nM range were incubated with 7.5 mM of PV for a reaction time up to 10 min at 37 °C (Fig. 3). h-BChE showed the greatest PVase activity, and h-AChE exhibited less PVase activity than h-BChE, but more than horse BChE and electric eel AChE.

The PVase activity of hAChE was linear and fell within the range of the tested enzyme concentrations.

Phenol formation by 5 nM of hAChE in the presence of 3 mM of PV was linear *versus* time within the range of 0–1200 s. The rate remained constant within the range of the tested times and, therefore, the assay was performed under steady-state conditions. However, phenol formation was linear within the range of 0–600 s in the presence of 0.25 mM PV. The rate remained constant and the steady state was reached within this time range.

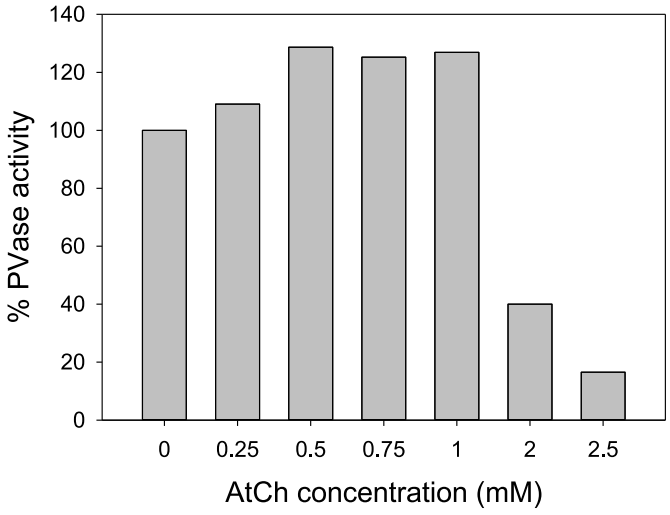

Fig. 5. Effects of AtCh concentrations with the PVase activity of hAChE. PVase activity was assayed with 3 mM PV for a 5-min reaction time at 37 °C at several AtCh concentrations.

Fig. 4 shows PV incubation at concentrations within the 0.250–8.000 mM range, with 5 nM of hAChE in the reaction volume (5-min reaction time), which yielded a behavior of a rectangular hyperbola and activity up to ~13 µM min^{-1} (up to 8 mM PV). Data were analyzed for all the enzymatic models available in the Enzyme Kinetic Module of the Sigma Plot software.

The best model that fitted to the data according to Akaike's criterion was the Michelis-Menten model in two independent experiments.

The K_M, Vmax and kcat values are provided in Fig. 4.

3.2. Interaction of acetylthiocholine with PVase activity

3.2.1. Competition between PV and AtCh

PVase activity was assayed in the presence of 0.5, 3 and 20 mM of

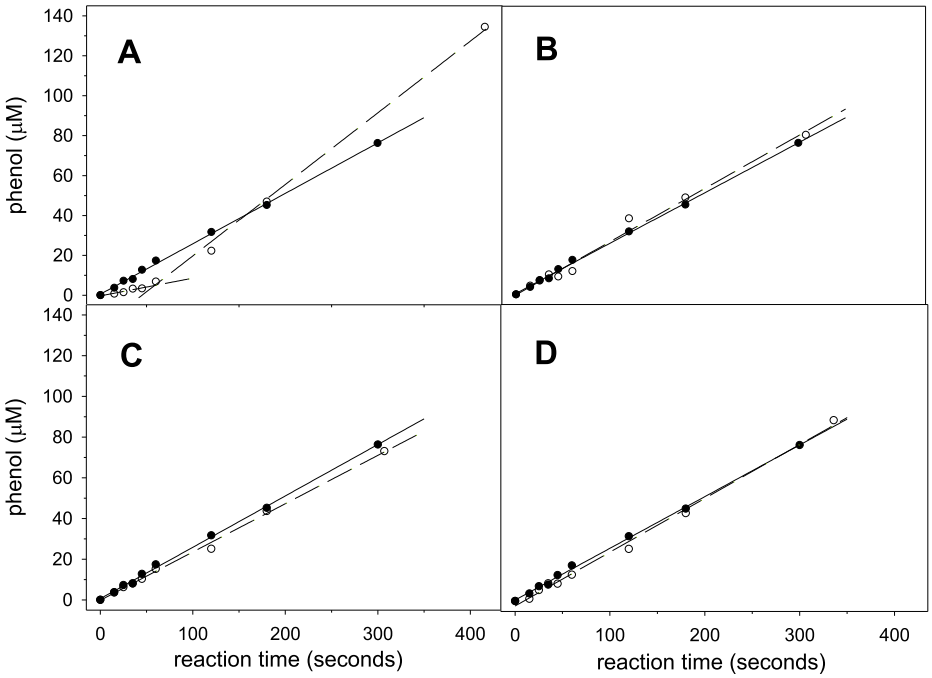

Fig. 6. - Time dependence of PVase activity in the absence and presence of AtCh, tCh, Ac or tCh and Ac. One example of the performed independent experiments is shown. Each point represents a triplicate measurement. 5 nM of hAChE (in reaction volume) in the presence of 3 mM of PV were assayed at different reaction times and 37 °C. Black circles represent phenol production in the absence of AtCh, tCh, Ac or tCh and Ac. Straight lines denote linear regression in all the panels. White circles indicate phenol production in the presence of 0.5 mM of AtCh (Panel A), 0.5 mM of tCh (Panel B), 0.5 mM of Ac (Panel C) and 0.5 mM of tCh and Ac (Panel D). Dashed lines depict linear regressions. Slopes (rates) are shown in Table 1.

Table 1
The estimated PVase activity rates of hAChE in the presence of cholinesterase substrate and its hydrolysis products: AtCh, tCh, Ac or tCh and Ac. Rates were estimated from the slopes obtained from the linear regressions of the experiments shown in Fig. 6.

Hydrolysis of PV by hAChE (n number of experiments) In the presence of	rate ± SD (Confidence Interval 95%)	
	First phase	Second phase
None (n = 16)	0.271 ± 0.068 (0.237–0.304) μM.sec^{-1}	
0.5 mM AtCh (n = 6)	0.074 ± 0.029 (0.05–0.09) μM.sec^{-1}	0.417 ± 0.090 (0.345–0.488) μM.sec^{-1}
0.75 mM AtCh (first phase, n = 6) (second phase, n = 7)	0.151 ± 0.072 (0.09–0.208) μM.sec^{-1}	0.490 ± 0.135 (0.390–0.589) μM.sec^{-1}
0.5 mM tCh (n = 4)	0.204 ± 0.048 (0.165–0.242) μM.sec^{-1}	
0.75 mM tCh (n = 2)	0.318 ± 0.071 (0.220–0.416) μM.sec^{-1}	
0.5 mM Ac (n = 2)	0.309 ± 0.010 (0.168–0.450) μM.sec^{-1}	
0.75 mM Ac (n = 2)	0.252 ± 0.066 (0.177–0.328) μM.sec^{-1}	
0.5 mM Ac + tCh (n = 5)	0.335 ± 0.043 (0.2.97–0.373) μM.sec^{-1}	
0.75 mM Ac + tCh (n = 2)	0.326 ± 0.141 (0.283–0.373) μM.sec^{-1}	

acetylthiocholine (AtCh), and was tested for PV as a substrate at the concentrations within the 0.25–8 mM range. Three independent experiments were performed.

The lowest AtCh concentration used in the experiments (0.5 mM) enhanced PVase activity, but higher AtCh concentrations competed with PV inhibiting the PVase activity (Fig. 4).

Effect of low and high AtCh concentrations on PVase activity.

Fig. 5 shows that PVase activity increased at low AtCh concentrations, and the greatest activity was reached at 0.5 mM AtCh under those assay conditions. However, PVase activity decreased at the highest AtCh concentrations.

3.2.2. *Effect of AtCh, thiocholine or acetate on PVase activity*

The PV hydrolysis time progression by hAChE was tested in the presence of 0.5 or 0.75 mM of AtCh, thiocholine (tCh), acetate (Ac) or tCh and Ac. PVase activity in the presence of AtCh (Fig. 6, Panel A) displayed two-step kinetic behavior: a lower rate than PVase activity in the absence of AtCh characterized the first phase (for short reaction times) and a higher rate than PVase activity in the absence of AtCh characterized the second phase. The theoretical inflection time was the reaction time at which both lines crossed and the slope changed (Fig. 6, panel A). It was estimated at around 49.60 ± 6.57 (mean ± SD) with a confidence interval (95%) of 43.16–56.04 (n = 4) for 0.5 mM of AtCh and 57.55 ± 5.69 (mean ± SD) with a Confidence Interval (95%) of 51.11–63.99 (n = 3) for 0.75 mM of AtCh.

No significant differences were observed between rates in the absence and presence of tCh, Ac or tCh and Ac (Fig. 6, Panels B, C and D).

The estimated kinetic parameters are shown in Table 1.

The PV hydrolysis time progression by hAChE was tested in the presence of 0.25 mM of phenylacetate. Phenylacetate was fully hydrolyzed in a reaction time of around 200–300 s (Fig. 7). The phenol production time progression in the presence of both substrates showed similar kinetic behavior to the phenylacetate hydrolysis in the absence of PV, but a linear increase in the phenol concentration was observed after a reaction time of 300 s (Fig. 7). This increase in phenol was produced by PV hydrolysis because phenylacetate was hydrolyzed almost completely after a reaction time of 300 s, and the slope (rate) of the linear regression from 300 s was 0.098 μM s^{-1}. The PV hydrolysis time progression in the absence of phenylacetate displayed a linear regression slope (rate) of 0.092 μM s^{-1}.

3.2.3. *Effect of AtCh on PVase activity*

Several AtCh concentrations were assayed in the presence of 3 mM of PV with 5 nM of hAChE in reaction volume. The results showed a dependence of the theoretical inflection time *versus* the AtCh concentration (Fig. 8; kinetic parameters are shown in Table 2).

No significant dependence on the rate of both phases was observed within the assayed concentrations range.

However, the theoretical inflection time showed linear dependence on the AtCh concentration (Fig. 9).

Similar results were obtained with an enzyme preparation of less

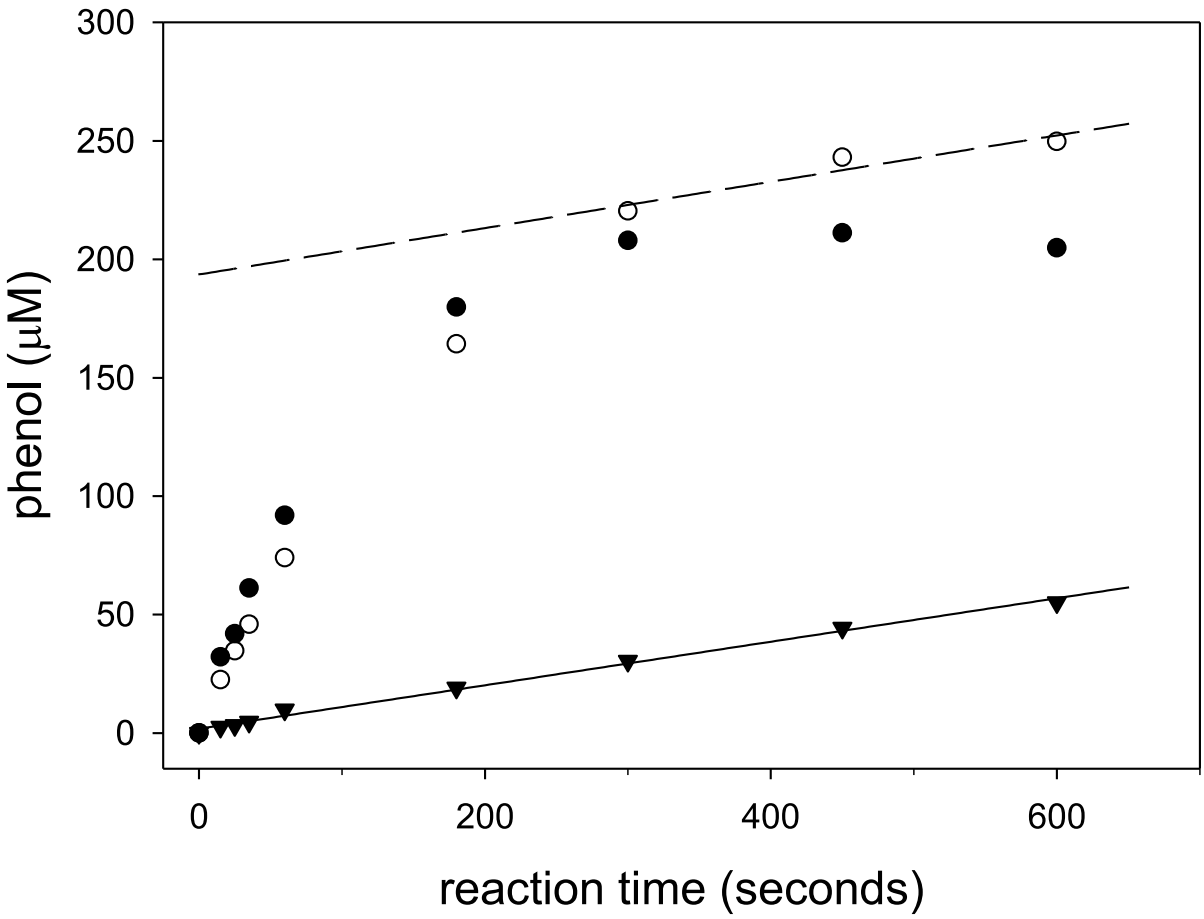

Fig. 7. - PVase activity time dependence in the absence and presence of phenylacetate. 5 nM of hAChE (in reaction volume) in the presence of 3 mM of PV or/and 0.25 mM of phenylacetate were assayed at different reaction times and 37 °C. Phenol production is represented in the presence of PV (black triangles), in the presence of phenylacetate (black circles) and in presence of PV and phenylacetate (white circles). The straight and dashed lines depict linear regression.

activity and at higher AtCh concentrations (see Figs. 1 and 2 and Table 1 in the Supplementary Material).

3.3. Interaction of acetylcholine with PVase activity

PVase activity in the presence of 1 mM of ACh or 1 mM of Ch showed a lower rate than PVase activity when both were absent (Fig. 10). PVase activity in the presence of ACh displayed two-step kinetic behavior: the first phase (with short reaction times) was characterized by a lower rate (0.045 μM s^{-1}) than the rates of PVase activity (0.155 μM s^{-1}) or PVase activity in the presence of Ch (0.08 μM s^{-1}); the second phase with a higher rate (0.119 μM s^{-1}) than PVase activity in the presence of Ch, but a lower rate than PVase activity. The theoretical inflection time was 41.62 s.

3.4. AtCh hydrolysis by hAChE

AtChE is the analog of the most commonly used physiological substrate to measure AChE. AtCh incubation at the concentrations within the 0.125–10000 mM range (with 0.05 nM of hAChE) yielded activity up to ~25 μM min^{-1} (with 1.5 mM of AtCh). Activity decreased at an AtCh concentration above 1.5 mM. The kcat estimated for a maximum rate was $4.48{\cdot}10^5 \pm 2.00{\cdot}10^5$ min^{-1} (mean ± SD) with a Confidence Interval (95%) of $2.22{\cdot}10^5$–$6.74{\cdot}10^5$ min^{-1} (n = 3). Fig. 11 shows the best fit according to Akaike's criterion. This was the biphasic substrate inhibition model (Fig. 1) in three experiments (Equation (1); with restriction Kss > Km).

The average values of Km, V1, V2 and Kss are provided in Table 3. The individual values of the kinetic parameters for each independent experiment are indicated in Supp. Table 2 in the Supplementary Material.

3.5. Interaction of PV with AtCh hydrolyzing activity

The AtCh hydrolyzing activity of 0.05 nM of hAChE in reaction volume was tested in the presence of 0.5, 3 and 8 mM of PV. The data revealed that AChE activity tended to reach a similar rate in the presence of all the PV concentrations and at high AtCh concentrations, which is a characteristic of a full competitive interaction. 3D data fits were done with the mathematical equation deduced from more than 80 different reversible inhibition models [33]. These model equations considered that the AtCh hydrolyzing activity of hAChE was inhibited by excess AtCh and, therefore, the different kinds of inhibition (full and partial competitive, full and partial uncompetitive, full and partial non competitive, full and partial mixed inhibitions) were contemplated in one phase or both phases of the biphasic substrate inhibition model shown by AtChE activity. All these models were evaluated by processing and analyzing data by adapting the model equation with the Enzyme Kinetic Module of the Sigma Plot.

The best-fitting model according to Akaike's criterion in three experiments was the model of full competitive inhibition in both phases according to the biphasic substrate inhibition (Equation (1), Fig. 1). The estimated kinetic parameters are indicated in Table 3. Panel A in Fig. 11 depicts the level curves obtained from the surface shown in Panel B at the employed PV concentrations.

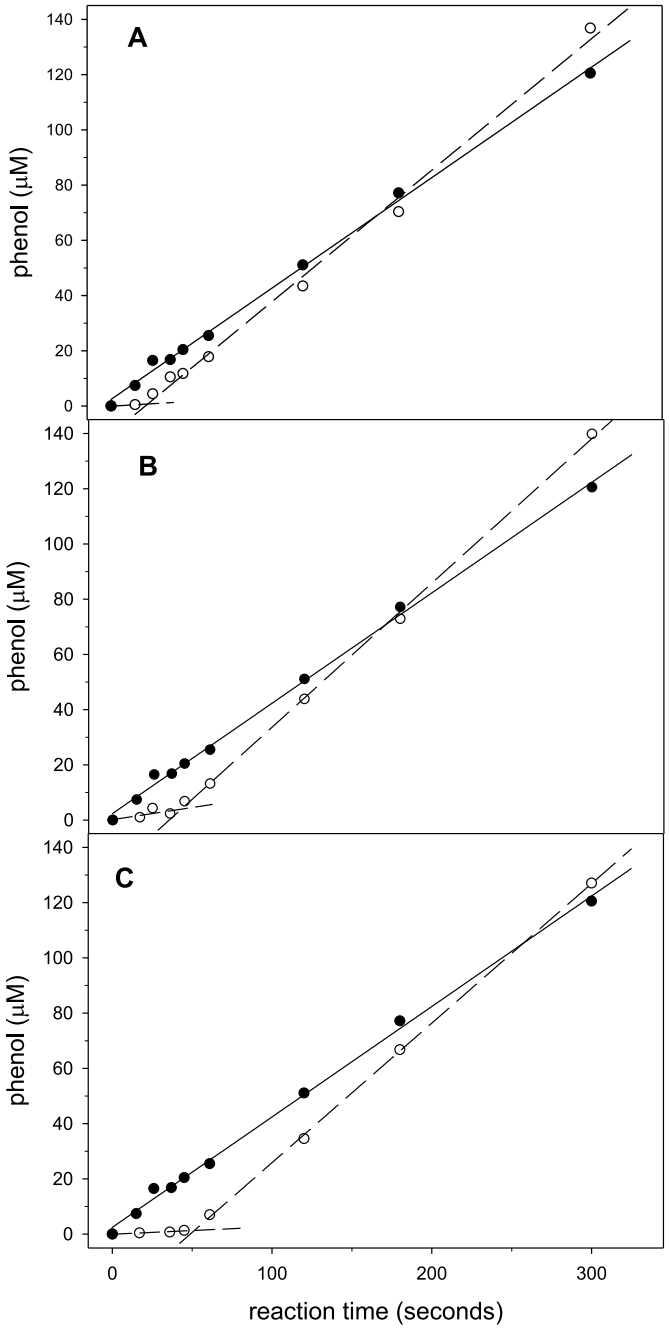

Fig. 8. - Interaction of AtCh with PVase activity. The enzyme reaction was performed with 3 mM of PV as the substrate (black circles) and in the presence of 0.25 (A), 0.5 (B), 0.75 (C) mM of AtCh in reaction volume.

Table 2
- Rates (slopes) and theoretical inflection times of PVase activity estimated in the presence of several AtCh concentrations. Parameters were estimated from the data shown in Fig. 8. The theoretical inflection time was the reaction time at which slopes theoretically changed.

Hydrolysis of PV by hAChE in presence of:	Fisrt phase rate (μM.sec^{-1})	Second phase rate (μM.sec^{-1})	Theoretical inflection time (sec)
0 nM AtCh	0.400		–
0.25 AtCh	0.034	0.476	22.93
0.50 AtCh	0.095	0.495	42.95
0.75 AtCh	0.027	0.510	51.42

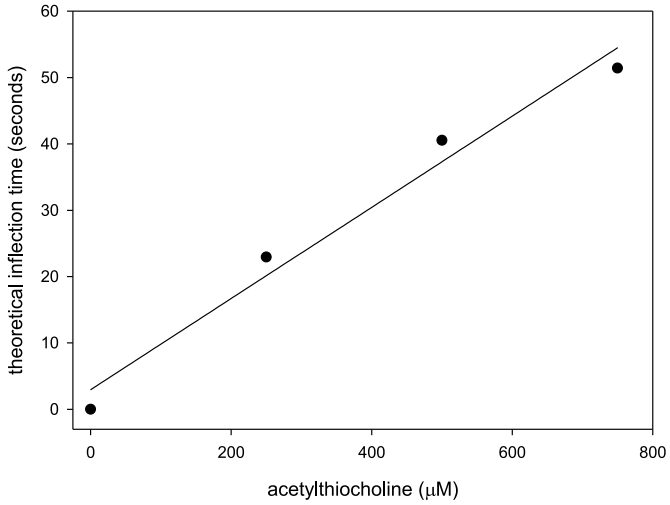

Fig. 9. - Dependence of the theoretical inflection time with the AtCh concentration. The shown data were obtained from Table 2. The linear regression parameters were y0 = 2.94 and m = 0.069.

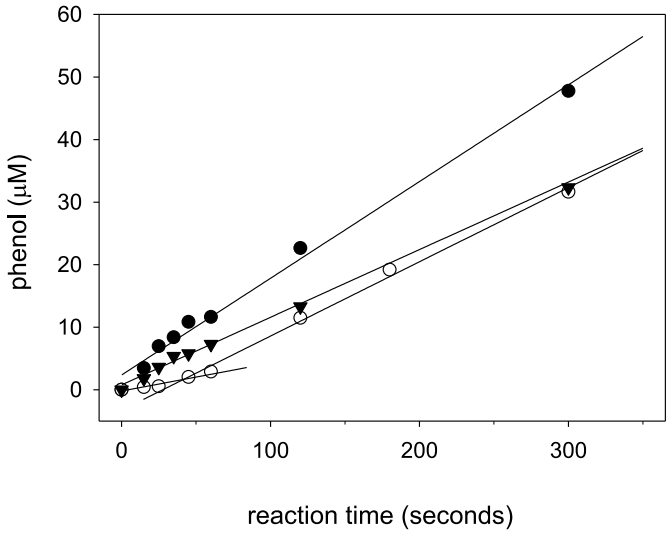

Fig. 10. - PVase activity time dependence in the absence and presence of ACh or Ch. 5 nM of hAChE in reaction volume was assayed at different reaction times. Black circles denote PV hydrolysis in the absence of ACh or Ch. White circles depict PV hydrolysis in the presence of 0.5 mM of ACh. Black triangles represent PV hydrolysis in the presence of 0.5 mM of Ch.

3.5.1. *Time progression of AtCh hydrolysis in the presence of PV*

The time progression of AtCh hydrolysis by 5 nM of hAChE in reaction volume was tested in the presence of 0.5 or 0.75 mM of AtCh. The AtCh hydrolysis results obtained in the presence of 0.5 or 0.75 mM of AtCh showed that AtCh was completely hydrolyzed in a reaction time of between 30 and 60 s (Fig. 12).

The time progression of 0.75 mM AtCh hydrolysis between 0 and 300 s by 5 nM of hAChE in reaction volume was tested in the presence of 3 mM of PV. No AChE activity inhibition was observed under these conditions.

4. Discussion

4.1. *PV hydrolysis by cholinesterases*

PVase activity was described in human butyrylcholinesterase (hBChE; [32,33]. Similarly, the data from this work (Fig. 3) indicated

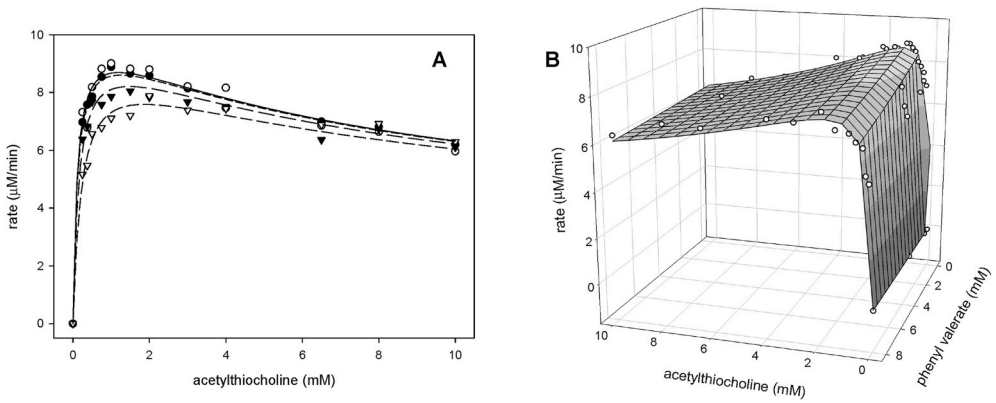

Fig. 11. ChE activity of hAChE in the presence of PV. One example of the three performed independent experiments is shown. AtCh concentrations (substrate): 0.125, 0.25, 0.375, 0.5, 0.75, 1, 2, 3, 4, 6.5, 8 and 10 mM. Inhibitor concentrations (PV): 0 (black circles), 0.5 (white circles), 3.0 (black triangles) and 8 mM (white triangles). Panel A indicates the level lines obtained from the 3D fit for each PV concentration and Panel B depicts the 3D fit.

Table 3
The AChE activity parameters estimated in the absence or presence of PV. The reactions of the kinetic models are shown in Figs. 1 and 2.

EXPERIMENT (n number of experiments))	Parameter ± SD (Confidence Interval 95%)
Hydrolysis of AtCh by hAChE (n = 3)	Km = 0.12 ± 0.02 (0.09–0,14) mM Kss = 8.9 ± 3.5 (4.9–12.8) mM V1 = 22.4 ± 10.0 (11.1–33.7) μM.min^{-1} V2 = 4.7 ± 1.6 (2.7–6.7) μM. min^{-1}
Interaction of PV with AtCh hydrolyzing activity. Full competitive inhibition (n = 3)	Km = 0.111 ± 0.004 (0.11–0.12) mM Kss = 10.5 ± 4.9 (5.0–16.1) mM K_{I1} = 6.3 ± 0.4 (5.8–6.7) mM K_{I2} = 1.6 ± 0.7 (0.8–2.4) mM V1 = 22.2 ± 10.2 (10.6–33.8) μM.min^{-1} V2 = 3.9 ± 4.3 (- 1–8.8) μM. min^{-1}

that hAChE possessed PVase activity and confirmed that PVase activity in cholinesterases depended on the species and the kind of cholinesterase, where hBChE displayed the greatest PVase activity and eeAChE the least.

4.2. PV hydrolysis by hAChE

This work revealed that the PVase activity behavior of hAChE was compatible with the Michaelis-Menten model. The Km constant herein estimated was similar to the Km shown in the literature for vinyl acetate, 1-butenylacetate, propylidene diacetate, 2-Acetaminoethyltrimethylammonium in eeAChE and phenyl acetate in electric eel and bovine erythrocytes (Table 4). The k_{cat} herein presented was similar to the k_{cat} estimated by the hydrolysis of butyrylthiocholine (Table 4) in mouse AChE and recombinant hAChE, which was two orders of magnitude lower than the k_{cat} for ACh and AtCh, and one order of magnitude lower than the k_{cat} for PV in hBChE [32,33].

4.3. Interaction of AtCh with PVase activity

The results of testing PVase in the presence of AtCh showed that PV and AtCh did not compete in a classic model of competition between substrates (Fig. 4). AtCh interacted with PVase activity in two different ways: at low and high AtCh concentrations. The interaction of AtCh at low concentrations (within the 0–1 mM range with 5 nM hAChE; Figs. 4 and 5) enhanced PVase activity and was compared in the absence of AtCh. However, the interaction of AtCh at high concentrations (within the 2–8 mM range with 5 nM of hAChE; Figs. 4 and 5) showed inhibited PVase activity. The PV hydrolysis time progression experiments in the absence or presence of 0.5 and 0.75 mM of AtCh indicated that the PV hydrolysis rate in the absence of AtCh remained constant within the assayed time range, but PV hydrolysis in the presence of AtCh showed two well-defined rates with short reaction times: the rate was lower than in the absence of AtCh; the rate for long reaction times (Fig. 6; Table 1)

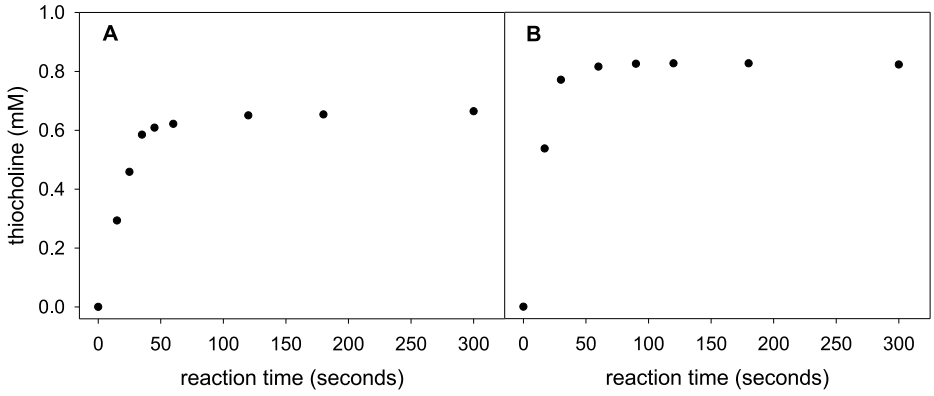

Fig. 12. - Time progression of AtCh hydrolysis in the presence of hAtChE. 5 nM of hAChE in reaction volume were assayed at different reaction times and 37 °C. Panel A shows the hydrolysis of 0.5 mM of AtCh. Panel B illustrates the hydrolysis of 0.75 mM of AtCh.

Table 4
Kinetic parameters for the substrates of AChE.

substrate	Specie/tissue	K_M (mM)	K_{SS} (mM)	k_{cat} (min^{-1})	Reference
Acetylcholine	electric eel	0.40	–	$9.8 \cdot 10^5$	[41]
	electric eel	–	–	$9.6 \cdot 10^5$	[42]
	bovine erythrocytes	0.15	–	–	[43]
	electric eel	0.085	–	$3.5 \cdot 10^5$	[44]
	bovine erythrocytes	3.20	–	–	[45]
	electric eel	–	–	$6.0 \cdot 10^5$	[46]
Acetylthiocholine	bovine erythrocytes	0.11	–	–	[43]
	human erythrocytes	0.058	18.6	$4.2 \cdot 10^5$	[47]
	bovine erythrocytes	0.11	14	–	[48]
	electric eel	0.21	–	–	[49]
	Mouse	0.046	15	$1.38 \cdot 10^5$	[50]
	recombinant-human	0.14	–	$3.7 \cdot 10^5$	[4]
	electric eel	67.0	–	$1.05 \cdot 10^6$	[41]
	Human	0.14	6	$4.0 \cdot 10^5$	[51]
Vinyl acetate	electric eel	1.10	–	$5.7 \cdot 10^5$	[41]
1-Butenylacetate	electric eel	1.70	–	$6.0 \cdot 10^5$	[41]
Propylidene diacetate	electric eel	1.50	–	$6.6 \cdot 10^5$	[41]
Benzylidene diacetate	electric eel	0.55	–	$10.2 \cdot 10^5$	[41]
Tropolone acetate	electric eel	2.50	–	$1.6 \cdot 10^4$	[41]
o-Nitro-chloroacetanilide	electric eel	0.60	–	$1.2 \cdot 10^4$	[41]
o-Nitro-dichloracetanilide	electric eel	–	–	$1.0 \cdot 10^6$	[42]
Phenyl acetate	bovine erythrocytes	2.6	–	–	[43]
	electric eel	0.87	–	$4.0 \cdot 10^5$	[44]
	electric eel	2	–	$7.5 \cdot 10^5$	[52]
	bovine erythrocytes	1.06	–	–	[45]
	bovine erythrocytes	1.31	–	–	[53]
	bovine erythrocytes	2.64	–	–	[48]
	electric eel	0.42	–	$1.44 \cdot 10^6$	[46]
	Eel	1.08	–	$4.88 \cdot 10^5$	[54]
	electric eel	–	–	$1.3 \cdot 10^5$	[42]
	electric eel	1.9	–	$9.9 \cdot 10^5$	[55]
Isoamyl acetate	bovine erythrocytes	5.81	–	–	[45]
	electric eel	–	–	$7.7 \cdot 10^4$	[42]
p-Nitrophenyl acetate	Mouse	4.3	–	$2.82 \cdot 10^4$	[50]
	recombinant-human	5.6	–	$1.1 \cdot 10^5$	[4]
o-nitrophenyl acetate	bovine erythrocyte	0.26	–	–	[56]
2-Acetaminoethyltrimethylammonium	Electric eel	1.1	–	216	[57]
7-acetoxy-*N*-methylquinolinium (M7A)	human erythrocyte	0.01	0.7	$7.8 \cdot 10^4$	[47]
indoxylacetate	electric eel	3.21	–	–	[49]
butyrylthiocholine	Mouse	0.093	7.1	$1.08 \cdot 10^3$	[50]
	recombinant-human	0.30	–	$7.5 \cdot 10^3$	[4]
	Human	0.30	3	$8.0 \cdot 10^3$	[51]
propionylthiocholine	Mouse	0.14	1.3	$1.38 \cdot 10^5$	[50]
	recombinant-human	0.25	–	$1.6 \cdot 10^5$	[4]
thiophenylacetate	Mouse	0.73	–	$1.38 \cdot 10^5$	[50]
S-3,3-Dimethylbutyl thioacetate	recombinant-human	0.45	–	$5.2 \cdot 10^4$	[4]
S-n-Propyl thioacetate	recombinant-human	11	–	$1.1 \cdot 10^4$	[4]

was higher than in the absence of AtCh. The theoretical reaction time during which the rate changed was herein defined as the theoretical inflection time (Fig. 6, Panel A; Fig. 8). This inflection time depended on the AtCh concentration, as Fig. 9 and Table 2 show. When the linear regression parameters of the inflection time data were taken into account (Fig. 9), the inflection time for the highest concentrations employed in the competition assay could be estimated (Fig. 4), which gave the values of 3.48 min and 9.22 min for 3 mM and 8 mM of AtCh, respectively. These estimated inflections could explain the inhibition at high AtCh concentrations because the reaction time of the competition assay (Fig. 4) was 5 min. Therefore, the rate in the first phase was the rate observed during almost all the reaction times in the presence of these AtCh concentrations.

The PV hydrolysis rates in the presence of 0.5 or 0.75 mM of Ac, tCh or Ac and tCh remained constant and were similar to the rates in the absence of these chemicals (Fig. 6, Panels B, C and D; Table 1). Therefore, no significant interaction with PVase activity was observed.

4.4. AtCh hydrolysis by hAChE

The results in Fig. 11 reveal that the model which best fitted the AtCh hydrolyzing activity (AtChE activity) data was the biphasic substrate inhibition model (Fig. 1, Equation (1); with restriction Kss > Km). The estimated kinetic parameters were similar to those estimated by Kaplan et al. [51] (Km = 0.14 mM, Kss = 6 mM, $k_{cat} = 4.0 \cdot 10^5$ min^{-1}) and Ordentlich et al. [4] (Km = 0.14 mM, $k_{cat} = 3.7 \cdot 10^5$ min^{-1}) for this kinetic model (Table 1). The interaction of PV and AtCh with hAChE was more complex than the competition between two substrates, where a biphasic substrate inhibition reaction occurred for one substrate (AtCh) and a Michaelis–Menten reaction for the other (PV). However, when considering PV to be an inhibitor [33,43], the AtChE activity kinetics in the presence of PV was compatible with the full competitive inhibition at a low AtCh concentrations and in excess of AtCh concentration (Fig. 11, Table 3). This kind of reversible inhibition occurs when the inhibitor interacts at the active site. The kinetic analysis suggested that PV inhibited the AtChE activity by interacting at the same active site as AtCh.

4.5. Effect of AtCh, tCh and Ac on PVase activity

No AChE activity inhibition (5 nM of AChE and 0.75 mM of AtCh) by 3 mM of PV was observed. Under these experimental conditions, 0.5 or 0.75 mM of AtCh was totally hydrolyzed between reaction times of 25–50 s (Fig. 12). According to these experiments, only AtCh affected

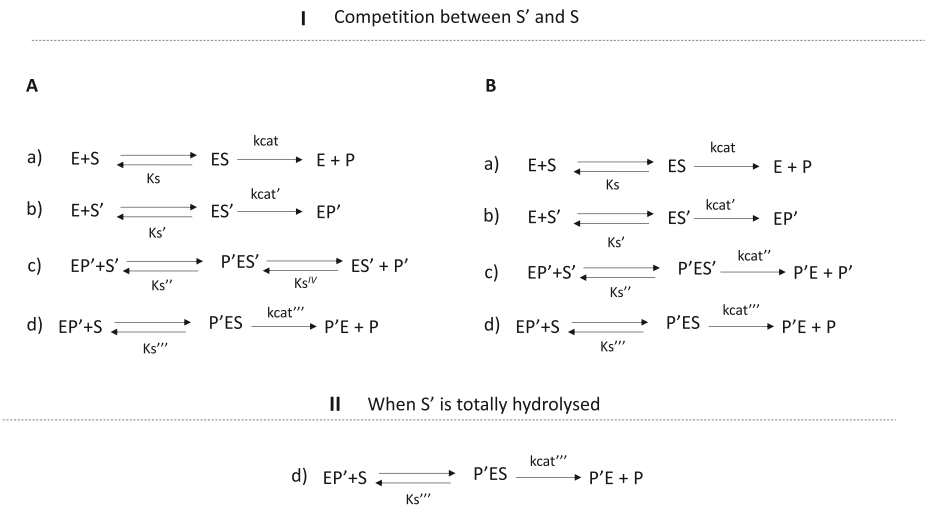

Fig. 13. - Proposed molecular mechanisms. S is substrate PV and S′ is substrate AtCh. P is phenol and P′ is tCh. I) Possible molecular mechanisms when S and S′ compete: A) P′ remains at the active site as S′ displaces it. B) P′ remains at the active site, but is not released to the reaction medium. II) One possible molecular mechanism is once S′ has been completely hydrolyzed, but excess S remains.

PVase activity for reaction times less than 25–50 s under these experimental conditions. Considering that the theoretical inflection times obtained in PV hydrolysis time progression experiments are between this range of time (Table 2), it is possible to deduce that these times indicate the theoretical times where AtCh would be totally hydrolyzed.

Therefore, the PV hydrolysis time progression experiments revealed that PVase activity was inhibited by AtCh until these inflections times and this activity was enhanced reaching higher activity than control activity after these inflection times (Fig. 6-Panel A and Fig. 8) once AtCh was completely hydrolyzed (Fig. 12).

This fact allowed us to deduce that PVase activity inhibition was managed by AtCh. However, it is very complicate to analyze this inhibition under the approach of classical competition between substrates [58], because it supposes that this competition is in the same active site, in steady state and with Michaelis-Menten behavior. In this work, it is difficult to assume that the kinetic behavior of PVase activity remains as Michaelis-Menten reaction in presence of AtCh and tCh, because, on the one hand, tCh activates the PVase activity and the interaction of the tCh in presence of AtCh is uncertain. On the other hand, AtCh inhibits while the kind of this interaction is unknown (either competitive, uncompetitive, non-competitive, or mixed inhibition). Furthermore, the rate of the AtCh hydrolysis did not remain constant in the experimental conditions of this work and therefore, the AtCh hydrolysis cannot be considered under steady state conditions.

The enhancement of PVase activity was managed by hydrolysis products tCh and Ac. Consequently, the inflection time increased with the rising AtCh concentration in the reaction medium (Fig. 8; Table 2). However, the PV hydrolysis time progression experiments done in the presence of tCh, Ac or tCh and Ac showed that the PVase activity rate did not significantly change (Fig. 6-Panels B, C and D; Table 1). This contradiction can be explained by considering that tCh and Ac interact differently when they were released by enzymatic activity (Fig. 6 Panel A) or they were previously in the reaction medium. The PV hydrolysis time progression experiment done in the presence of phenylacetate (Fig. 7) showed that the Ac released by enzymatic activity did not enhance PVase activity because once phenylacetate had completely hydrolyzed, the phenol production rate (linear regression slope) was similar to the PVase activity rate in the absence of phenylacetate.

Rosenberry and coworkers demonstrated that PAS in AChE can trap the substrate and other ligands, and that the ligand binding to the PAS can cause a steric blockade of the esteratic site or an allosteric activation [59]. PAS shows a low affinity for AtCh and the inhibition by excess of AtCh is observed at higher concentrations than 1 mM (Fig. 11; [59]. Therefore, no significant interaction in the PAS and no allosteric inhibition is expected in this work because AtCh concentrations used were sub-milimolar. For this reason, we can approach that the inhibition PVase activity is mostly related to the competition between substrates in the active site, and therefore substrates would alter the last step of the crosstalk from the PAS to the active center. It is not possible to discard that an inhibition caused by PAS interactions can be taking place at higher concentrations of AtCh. The PAS is localized on the AChE surface around the cavity entrance, then only the tCh released to reaction medium could interact with the PAS, but no effect was observed on the PVase activity (Fig. 6, Panel B).

The data herein obtained suggest that after hydrolysis of AtCh some molecules of tCh interact and could remain reversibly or irreversibly bound in some place of the active site, even after AtCh had been totally hydrolyzed, modifying the PVase activity. Hence, AtCh would behave like a Trojan Horse because it would allow products to be released at the active site and would avoid the barriers that these products could face if they were in the reaction medium. Further studies are needed to better understand the role of AtCh and tCh in these experimental conditions.

4.6. *Interaction of ACh with PVase activity*

The PV hydrolysis time progression experiments done in the presence of 1 mM of ACh or the presence of 1 mM of Ch obtained lower rates than the rates acquired in the absence of ACh (Fig. 10). An inflection time of around 42 s was observed during the PV hydrolysis time progression experiments in the presence of ACh, which indicated that PVase activity was inhibited by ACh. The PV hydrolysis rate in the presence of Ch was constant and lower than that noted in the second phase in the presence of ACh (Fig. 10), which indicated that PVase activity was activated by the Ch released at the active site once ACh had been completely hydrolyzed. The fact that this activated activity showed a lower rate than the activity in the absence of ACh could be explained by considering that the Ch released to the reaction medium would inhibit PVase activity. Then Ch could activate and inhibit PVase activity at the same time, the Ch released to reaction medium would inhibit the PVase activity and the Ch released to the active site would enhance this activity.

4.7. Other considerations related to PV-AtCh interactions in hAChE

tCh plays an important role in PVase activity when it is released from AtCh. According to the results obtained with this work, it is possible to deduce at least two possible reaction mechanisms (shown in Fig. 13) that could explain the observations of this work. As indicated by reactions b) and c) in Fig. 13-Panel A, P' (tCh) would remain at the active site until S' enters (AtCh) and moves it toward the reaction medium. Another possible mechanism is shown in reactions b) and c) in Fig. 13-Panel B, where tCh could also interact with AChE activity, and remain at the active site and transform the enzyme into an activated enzyme.

Other substrates (including biological substrates) could interact similarly by conferring the hAChE property of being more effective in hydrolyzing a substrate in the presence of tCh or another substrate product once this substrate has been completely hydrolyzed.

5. Overall remarks and conclusions

hAChE cannot be excluded from the pool of OP-sensitive proteins with PVase activity. PV and AtCh are hydrolyzed at the same time. The results show that the interaction between both substrates is not compatible to a simple competition model between the substrates at the same active site. The interaction of AtCh in PVase activity is not a competitive reversible inhibition at the same active site. PVase activity increases when tCh is released at the active site in the presence of AtCh and once AtCh has been completely hydrolyzed. Considering all the results on the whole, we conclude that the interactions between both substrates in hAChE are compatible with a more complex interaction for each substrate. ACh interacts with PVase activity, similarly to the interaction of AtCh, but in this case Ch released to the reaction medium inhibits PVase activity. The products released at the active site could play an important role in the hydrolysis reactions of different substrates in biological systems. Further research is needed to understand the improvement and inhibition of the PVase activity in presence of AtCh. This will help to understand the role in the kinetics with substrates, inhibitors and the catalytic process in toxicity.

Declaration of competing interest

The authors declare that they have no known competing financial interests or personal relationships that could have appeared to influence the work reported in this paper.

Appendix A. Supplementary data

Supplementary data related to this article can be found at https://doi.org/10.1016/j.cbi.2021.109764.

References

[1] I. Mangas, J. Estévez, E. Vilanova, T.C. Costa Franca, New insights on molecular interactions of organophosphorus pesticides with esterases, Toxicology 376 (2017) 30–43.

[2] E.A. Barnard, Enzymatic destruction of acetylcholine, in: J.I. Hubbard (Ed.), The Peripheral Nervous System, Plenum Publishers, New York, 1974, p. 201 224.

[3] H. Dvir, I. Silman, M. Harela, T.L. Rosenberry, J.L. Sussman, Acetylcholinesterase: from 3D structure to function, Chem. Biol. Interact. 187 (1–3) (2010) 10–22.

[4] A. Ordentlich, D. Barak, C. Kronman, Y. Flashner, M. Leitner, Y. Segall, N. Ariel, S. Cohen, B. Velan, A. Shafferman, Dissection of the human acetylcholinesterase active center determinants of substrate specificity. Identification of residues constituting the anionic site, the hydrophobic site, and the acyl pocket, J. Biol. Chem. 268 (23) (1993) 17083–17095.

[5] V. Tõugu, Acetylcholinesterase: mechanism of catalysis and inhibition, Curr. Med. Chem. Cent. Nerv. Syst. Agents 1 (2001) 155–170.

[6] I.B. Wilson, F. Bergmann, Acetylcholinesterase. VIII. Dissociation constants of the active groups, J. Biol. Chem. 186 (2) (1950) 683–692.

[7] I. Silman, J.L. Sussman, Acetylcholinesterase: 'classical' and 'non-classical' functions and pharmacology, Curr. Opin. Pharmacol. 5 (3) (2005) 293–302.

[8] I. Silman, J.L. Sussman, Acetylcholinesterase: how is structure related to function? Chem. Biol. Interact. 175 (1–3) (2008) 3–10.

[9] S. Shakil, R. Khan, S. Tabrez, Q. Alam, N.R. Jabir, M.I. Sulaiman, N.H. Greig, M. A. Kamal, Interaction of human brain acetylcholinesterase with cyclophosphamide: a molecular modeling and docking study, CNS Neurol. Disord. - Drug Targets 10 (7) (2011) 845–848.

[10] J.L. Sussman, I. Silman, Acetylcholinesterase: structure and use as a model for specific cation-protein interactions, Curr. Opin. Struct. Biol. 2 (1992) 721–729.

[11] A. Ordentlich, D. Barak, C. Kronman, N. Ariel, Y. Segall, B. Velan, A. Shafferman, Functional characteristics of the oxyanion hole in human acetylcholinesterase, J. Biol. Chem. 273 (31) (1998) 19509–19517.

[12] M. Pohanka, Cholinesterases, a target of pharmacology and toxicology, Biomed. Pap. Med. Fac. Univ. Palacky. Olomouc. Czech. Repub. 155 (3) (2011) 219–229.

[13] J.L. Sussman, M. Hare, F. Frolow, C. Oefner, A. Goldman, L. Toker, I. Silman, Atomic structure of acetylcholinesterase from Torpedo Californica: a prototypic acetylcholine-binding protein, Science 253 (5022) (1991) 872–879.

[14] G. Johnson, S.W. Moore, The peripheral anionic site of acetylcholinesterase: structure, functions and potential role in rational drug design, Curr. Pharmaceut. Des. 12 (2) (2006) 217–225.

[15] W.D. Mallender, T. Szegletes, T.L. Rosenberry, Acetylthiocholine Binds to asp74 at the Peripheral site of human acetylcholinesterase as the first step in the catalytic pathway, Biochemistry 39 (26) (2000) 7753–7763.

[16] A. Shafferman, B. Velan, A. Ordentlich, C. Kronman, H. Grosfeld, M. Leitner, Y. Flashner, S. Cohen, D. Barak, N. Ariel, Substrate inhibition of acetylcholinesterase: residues affecting signal transduction from the surface to the catalytic center, EMBO J. 11 (10) (1992) 3561–3568.

[17] M.K. Johnson, Structure-activity relationships for substrates and inhibitors of hen brain neurotoxic esterase, Biochem. Pharmacol. 24 (7) (1975) 797–805.

[18] J.M. Chemnitius, K.H. Haselmeyer, R. Zech, Neurotoxic esterase. Identification of two isoenzymes in hen brain, Arch. Toxicol. 53 (3) (1983) 235–244.

[19] C.D. Carrington, M.B. Abou-Donia, The correlation between the recovery rate of neurotoxic esterase activity and sensitivity to organophosphorus-induced delayed neurotoxicity, Toxicol. Appl. Pharmacol. 75 (2) (1984) 350–357.

[20] E. Vilanova, J. Barril, V. Carrera, M.C. Pellin, Soluble and particulate forms of the organophosphorus neuropathy target esterase in hen sciatic nerve, J. Neurochem. 55 (4) (1990) 1258–1265.

[21] P. Glynn, D.J. Read, R. Guo, S. Wylie, M.K. Johnson, Synthesis and characterization of a biotinylated organophosphorus ester for detection and affinity purification of a brain serine esterase: neuropathy target esterase, Biochem. J. 301 (2) (1994) 551–556.

[22] P. Glynn, J.L. Holton, C.C. Nolan, D.J. Read, L. Brown, A. Hubbard, J.B. Cavanagh, Neuropathy target esterase: immunolocalization to neuronal cell bodies and axons, Neuroscience 83 (1) (1998) 295–302.

[23] M.V. Céspedes, M.A. Escudero, J. Barril, M.A. Sogorb, J.L. Vicedo, E. Vilanova, Discrimination of carboxylesterases of chicken neural tissue by inhibition with a neuropathic, non-neuropathic organophosphorus compounds and neuropathy promoter, Chem. Biol. Interact. 106 (3) (1997) 191–200.

[24] M.A. Escudero, M.V. Céspedes, E. Vilanova, Chromatographic discrimination of soluble neuropathy target esterase isoenzymes and related phenyl valerate esterases from chicken brain, spinal cord, and sciatic nerve, J. Neurochem. 68 (5) (1997) 2170–2176.

[25] J. Barril, J. Estévez, M.A. Escudero, M.V. Céspedes, N. Níguez, M.A. Sogorb, A. Monroy, E. Vilanova, Peripheral nerve soluble esterases are spontaneously reactivated after inhibition by paraoxon: implications for a new definition of neuropathy target esterase, Chem. Biol. Interact. 119 (120) (1999) 541–550.

[26] J. Estévez, A. García-Perez, J. Barril, M.C. Pellín, E. Vilanova, The inhibition of the hight sensitive peripheral nerve soluble esterases by mipafox. A new mathematical processing for the kinetics of inhibition of esterases by organophosphorus compounds, Toxicol. Lett. 151 (2004) 243–249.

[27] J. Estévez, J. Barril, E. Vilanova, Inhibition with spontaneous reactivation and the "ongoing inhibition" effect of esterases by biotinylated organophosphorus compounds: S9B as a model, Chem. Biol. Interact. 187 (1–3) (2010) 397–402.

[28] J. Estévez, A. García-Pérez, J. Barril, E. Vilanova, Inhibition with spontaneous reactivation of carboxyl esterases by organophosphorus compounds: paraoxon as a model, Chem. Res. Toxicol. 24 (1) (2011) 135–143.

[29] I. Mangas, E. Vilanova, J. Estévez, Kinetics of the inhibitory interaction of organophosphorus neuropathy inducers and non-inducers in soluble esterases in the avian nervous system, Toxicol. Appl. Pharmacol. 256 (2011) 360–368.

[30] M. Benabent, E. Vilanova, M.A. Sogorb, J. Estévez, Cholinesterase assay by an efficient fixed time endpoint method, MethodsX 1 (2014) 258–263.

[31] I. Mangas, Z. Radić, P. Taylor, M. Ghassemian, H. Candela, E. Vilanova, J. Estévez, Butyrylcholinesterase identification in a phenylvalerate esterase-enriched fraction sensitive to low mipafox concentrations in chicken brain, Arch. Toxicol. 91 (2) (2017) 909–919.

[32] I. Mangas, E. Vilanova, J. Estévez, Phenyl valerate esterase activity of human butyrylcholinesterase, Arch. Toxicol. 91 (2017) 3295–3305.

[33] J. Estévez, F. Rodrigues de Souza, M. Romo, I. Mangas, T.C. Costa Franca, E. Vilanova, Interactions of human butyrylcholinesterase with phenylvalerate and acetylthiocholine as substrates and inhibitors: kinetic and molecular modeling approaches, Arch. Toxicol. 93 (5) (2019) 1281–1296.

[34] M.K. Johnson, Improved assay of neurotoxic esterase for screening organophosphates for delayed neurotoxicity potential, Arch. Toxicol. 37 (2) (1977) 113–115.

[35] X.Q. Li, T.B. Andersson, M. Ahlström, L. Weidolf, Comparison of inhibitory effects of the proton pump-inhibiting drugs omeprazole, esomeprazole, lanso-prazole, pantoprazole and rabeprazole on human cytochrome P450 activities, Drug Metab. Dispos. 32 (2004) 821–827.

[36] Z. Fišar, J. Hroudová, J. Raboch, Inhibition of monoamine oxidase activity by antidepressants and moodstabilizers, Neuroendocrinol. Lett. 31 (5) (2010) 645–656.
[37] B. Calamini, K. Ratia, M.G. Malkowski, M. Cuendet, J.M. Pezuto, B.D. Santarsiero, A.D. Mesecar, Pleiotropic mechanisms facilitated by resveratrol and its metabolites, Biochem. J. 429 (2010) 273–282.
[38] Z. Radić, N.A. Pickering, D.C. Vellom, S. Camp, P. Taylor, Three distinct domains in the cholinesterase molecule confer selectivity for acetyl- and butyrylcholinesterase inhibitors, Biochemistry 32 (45) (1993) 12074–12084.
[39] G. Cauet, A. Friboulet, D. Thomas, Horse serum butyrylcholinesterase kinetics: a molecular mechanism based on inhibition studies with dansylaminoethyltrimethylammonium, Biochem. Cell. Biol. 65 (6) (1987) 529–535.
[40] P. Masson, S. Adkinst, P. Gouet, O. Lockridge, Recombinant human butyrylcholinesterase G390V, the fluoride-2 variant, expressed in Chinese hamster ovary cells, is a low affinity variant, J. Biol. Chem. 268 (19) (1993) 14329–14341.
[41] M. Naveh, Z. Bernstein, D. Segal, Y. Shalitin, New substrates of acetylcholinesterase, FEBS Lett. 134 (1) (1981) 53–56.
[42] T.L. Rosenberry, Catalysis by Acetylcholinesterase: evidence that the rate-limiting step for acylation with certain substrates precedes general acid-base catalysis, Proc. Natl. Acad. Sci. U.S.A. 72 (10) (1975) 3834–3838.
[43] E. Reiner, V. Simeon, Competition between substrates for acetylcholinesterase and cholinesterase, Biochim. Biophys. Acta 480 (1) (1977) 137–142.
[44] R. Durán, C. Cerveñansky, F. Dajas, K.F. Tipton, Fasciculin inhibition of acetylcholinesterase is prevented by chemical modification of the enzyme at a peripheral site, Biochim. Biophys. Acta 1201 (3) (1994) 381–388.
[45] R.M. Krupka, Hydrolysis of neutral substrates by acetylcholinesterase, Biochemistry 5 (6) (1966) 1983–1988.
[46] I.M. Kovach, M. Larson, R.L. Schowen, One-proton catalysis in the deacetylation of acetylcholinesterase, J. Am. Chem. Soc. 108 (1986) 3054–3056.
[47] T. Szegletes, W.D. Mallender, P.J. Thomas, T.L. Rosenberry, Substrate binding to the peripheral site of acetylcholinesterase initiates enzymatic catalysis. Substrate inhibition arises as a secondary effect, Biochemistry 38 (1) (1999) 122–133.
[48] E. Reiner, V. Simeon, Kinetic study of the effect of substrates on reversible inhibition of cholinesterase and acetylcholinesterase by two coumarin derivatives, Croat. Chem. Acta 47 (1975) 321–331.
[49] M. Pohanka, M. Hrabinova, K. Kuca, J.P. Simonato, Assessment of acetylcholinesterase activity using indoxylacetate and comparison with the standard ellman's method, Int. J. Mol. Sci. 12 (2011) 2631–2640.
[50] Z. Radić, P. Taylor, Interaction kinetics of reversible inhibitors and substrates with acetylcholinesterase and its fasciculin 2 complex, J. Biol. Chem. 276 (7) (2001) 4622–4633.
[51] D. Kaplan, A. Ordentlich, D. Barak, N. Ariel, C. Kronman, B. Velan, A. Shafferman, Does "butyrylization" of acetylcholinesterase through substitution of the six divergent aromatic amino acids in the active center gorge generate an enzyme mimic of butyrylcholinesterase? Biochemistry 40 (25) (2001) 7433–7445.
[52] H.C. Froede, I.B. Wilson, The slow rate of inhibition of acetylcholinesterase by fluoride, Mol. Pharmacol. 27 (6) (1985) 630–633.
[53] R.M. Krupka, Acetylcholinesterase: trimethylammonium-ion inhibition of deacetylation, Biochemistry 3 (1964) 1749–1754.
[54] G.M. Steinberg, N.C. Thomas, M.L. Mednick, J.W. Amshey Jr., Acetylcholinesterase substrates: acetoxymethylpyridines and benzyl acetate, J. Pharmacol. Sci. 61 (11) (1972) 1735–1738.
[55] M.L. Bender, M.L. Begué-Cantón, R.L. Blakeley, L.J. Brubacher, J. Feder, C. R. Gunter, F.J. Kézdy, J.V. Killheffer Jr., T.H. Marshall, C.G. Miller, R.W. Roeske, J. K. Stoops, The determination of the concentration of hydrolytic enzyme solutions: alpha-chymotrypsin, trypsin, papain, elastase, subtilisin, and acetylcholinesterase, J. Am. Chem. Soc. 88 (24) (1966) 5890–5913.
[56] R.M. Krupka, F.L. Hastings, A.R. Main, F. Iverson, Nitrophenyl acetate hydrolysis by acetylcholinesterase. A Correction, J. Agric. Food Chem. 22 (1974) 6.
[57] D.E. Moore, G.P. Hess, Acetylcholinesterase-catalyzed hydrolysis of an amide, Biochemistry 14 (11) (1975) 2386–2389.
[58] G. Waley, Kinetic parameters from progress curves of competing substrates. Application to beta-lactamases, Biochem. J. 211 (1983) 511–513.
[59] T.L. Rosenberry, J.L. Johnson, B. Cusack, J.L. Thomas, S. Emani, K. S. Venkatasubban, Interactions between the peripheral site and the acylation site in acetylcholinesterase, Chem. Biol. Interact. 157–158 (2005) 181–189.